

# DATA ASYMMETRY ANALYSIS FOR SPACE SHUTTLE COMMUNICATIONS LINK

**M. K. Simon**  
Jet Propulsion Lab  
Pasadena, California 91103

**K. Tu**  
Lockheed Electronics Company, Inc.  
Houston, Texas 77058

**B. H. Batson**  
NASA Lyndon B. Johnson  
Space Center  
Houston, Texas 77058

## ABSTRACT

This paper systematically analyzes the signal-to-noise ratio degradations which can potentially occur due to data asymmetry in digital transmission systems. Suitable asymmetry models are developed and error probability performance for two types of data detectors (integrate-and-dump filter, and gated-integrate-and-dump filter) is derived. Although this work was done to resolve problems being encountered in the Shuttle Ku-band return link design, specifically for the 50 Mbps convolutionally encoded channel (NRZ format), generalizations are made which provide results for other cases of interest (other Ku-band return link channels, or other systems entirely). This paper therefore considers Manchester data formats (in addition to NRZ) and uncoded transmission (in addition to convolutionally coded transmission).

## INTRODUCTION

The Shuttle Ku-band return link mode 1 (PM) [1] is used to transmit: 1) convolutionally encoded (rate 1/2, constraint length 7) payload data with data rates up to 50 Mbps (NRZ format), 2) 192 Kbps uncoded Orbiter operational data (Manchester format), and 3) one of a variety of other sources, including medium rate coded or uncoded data with data rate up to 2 Mbps (NRZ) or 1 Mbps (Manchester). A generalization of the basic QPSK technique is employed for modulation of these three data channels onto quadrature carriers [2]. An area of concern in the development of the Ku-band system arose over the data asymmetry in the 50 Mbps channel produced by differential propagation delays through logic circuits in the payloads and also in the Orbiter Ku-band signal processor for rising and falling voltage transitions. This data asymmetry was potentially capable of causing a severe performance degradation to the demodulated data at the TDRSS (Tracking and Data Relay Satellite System) ground station.

This paper develops suitable asymmetry models and determines the amount of channel performance degradation as a function of the amount of data asymmetry.

Specifically, we first present two asymmetry models which accurately describe the physical sources from which asymmetry originates. Following this, we present, for both NRZ and Manchester data, the error probability performance corresponding to various types of data detectors (with or without d.c. restoration) including the integrate-and-dump filter and gated-integrate-and-dump filter. Detailed performance analyses for these various cases may be found in [3] and [4].

## ASYMMETRY MODELS AND DEFINITIONS

To quantitatively determine the degrading effect of data asymmetry on error rate performance, one must develop a suitable asymmetry model which accurately describes the physical source from which the asymmetry originates. It was determined that two possible models are appropriate and, provide that asymmetry is properly defined, either model produces the identical performance degradation due to this asymmetry. In the first model, the assumption is made that +1 NRZ symbols are elongated by  $\Delta T/2$  (relative to their nominal value of T sec) when a negative-going data transition occurs and -1 symbols are shortened by the same amount when a positive-going data transition occurs.\* Otherwise (when no transitions occur), the symbols maintain their nominal T sec width. Thus,  $\Delta T$  represents the relative difference in length between the elongated +1 and shortened -1 symbols. An example demonstrating this model is illustrated in Figure 1b. The second asymmetry model makes the assumption that positive NRZ pulses are lengthened whenever adjacent pulses are negative. Thus, a given positive pulse preceded and succeeded by a negative pulse would be increased in duration at both ends. Stated another way, a positive-going transition occurs early and a negative-going transition occurs late relative to the nominal transition time instants. Letting  $\delta$  represent the fractional (relative to the nominal bit duration T) increase in positive pulse length due to a single adjacent negative pulse, then for a given random data sequence, the shortest pulse would have length  $T(1-2\delta)$ , while the longest would have length  $T(1+2\delta)$ . Figure 1c illustrates the application of the second asymmetry model to the same bit stream as that used in Figure 1b.

Regardless of which asymmetry model is used, data asymmetry is defined as the difference in length between the shortest and longest pulses in the sequence divided by their sum. For the first model, this definition gives

$$\text{Asymmetry } \underline{\Delta}_n = \frac{T(1 + \frac{\Delta}{2}) - T(1 - \frac{\Delta}{2})}{T(1 + \frac{\Delta}{2}) + T(1 - \frac{\Delta}{2})} = \frac{\Delta}{2}, \quad (1)$$

---

\* Due to symmetry in the data itself, it is immaterial whether the elongated pulse is of positive or negative polarity, and vice versa for the shortened pulse.

whereas for the second model, we get

$$\eta = \frac{T(1+2\delta) - T(1-2\delta)}{T(1+2\delta) + T(1-2\delta)} = 2\delta. \quad (2)$$

In the absence of noise, the timing instants (i.e., the epochs of the symbol synchronization clock) for the recovered data clock (assuming random data) will occur, for the first asymmetry model, at  $t = T(n + \frac{\Delta}{4})$ ;  $n = 0, \pm 1, \pm 2, \dots$ . For the second model, it can easily be shown that, on the average, the symbol synchronizer will lock up at the nominal transition points of the equivalent symmetric data waveform (as shown in Figure 1a), i.e.,  $0, \pm T, \pm 2T, \pm 3T, \dots$

In this paper, the first model is adopted for purposes of analysis.

### **ERROR PROBABILITY PERFORMANCE (Integrate and dump detector, NRZ signal)**

When an integrate and dump filter is used for detection of random NRZ data (50% transition density) with asymmetry, then the in-phase integrate-and-dump output depends, in general, on the polarity of the symbol over which it is integrating and that of the preceding and succeeding symbols. Thus, one must compute the in-phase integrate-and-dump output for each of the eight possible three-symbol sequences and their corresponding conditional error probabilities. Then averaging these conditional error probabilities over the eight equally-likely three-symbol sequences gives the average error probability  $P_E$ , i.e.,

$$\begin{aligned} P_E &= \frac{1}{8} \left\{ 5 \left[ \frac{1}{2} \operatorname{erfc} \sqrt{E_s/N_0} \right] + 2 \left[ \frac{1}{2} \operatorname{erfc} \left( \sqrt{E_s/N_0} \left( 1 - \frac{\Delta}{2} \right) \right) \right] + \frac{1}{2} \operatorname{erfc} \left( \sqrt{E_s/N_0} \left( 1 - \Delta \right) \right) \right\} \\ &= \frac{5}{16} \operatorname{erfc} \sqrt{E_s/N_0} + \frac{1}{8} \operatorname{erfc} \left[ \sqrt{E_s/N_0} \left( 1 - \eta \right) \right] + \frac{1}{16} \operatorname{erfc} \left[ \sqrt{E_s/N_0} \left( 1 - 2\eta \right) \right] \quad (3) \end{aligned}$$

where  $E_s$  denotes the symbol energy,  $N_0$  the channel noise spectral density, and

$$\operatorname{erfc} x \triangleq \frac{2}{\sqrt{\pi}} \int_x^{\infty} e^{-t^2} dt. \quad (4)$$

The signal-to-noise ratio (SNR) degradations can then be obtained from (3) by computing the additional  $E_s/N_0$  required ( $\Delta E_s/N_0$ ) due to asymmetry to produce the same value of symbol error probability when  $\eta = 0$ , i.e.,  $P_E^0$ , where

$$P_E^0 \triangleq \frac{1}{2} \operatorname{erfc} \sqrt{E_s/N_0} \quad (5)$$

Table 1 gives these degradations in dB for uncoded random NRZ data.

For a convolutionally encoded signal, an exact analysis is not tractable. However, we can approximately obtain the SNR degradation from the decoder bit error performance curve and equations (3) and (5) by assuming that the coding is transparent to the asymmetry and using the uncoded symbol energy-to-noise ratios corresponding to the coded bit energy-to-noise density ratios at the desired bit error rates. Table 2 contains the symbol energy-to-noise density ratio degradations (in dB) for asymmetry values  $n \times 100\%$  of 3, 7, 10, 15 and 20% and  $E_s/N_o = 0, 0.8, \text{ and } 1.5$  dB. The values of  $E_s/N_o$  selected correspond to bit energy-to-noise density ratios  $E_b/N_o = 3, 3.8$  and  $4.5$  dB which, respectively, correspond to Viterbi decoder bit error probabilities  $P_b = 10^{-3}, 10^{-4}, \text{ and } 10^{-5}$  (for rate  $1/2$ , constraint length 7). From Table 2, it should be noted that error probability performance for the coded signal is relatively insensitive to data asymmetry.

### **ERROR PROBABILITY PERFORMANCE (Integrate-and-Dump Detector, Manchester Signal)**

Although Manchester coding is not employed on the Shuttle Ku-band high rate channel (50 Mbps) because of bandwidth limitations on the Ku-band return link, such coding is sometimes used on the lower rate channels [1], and thus the effect of asymmetry on the performance of these channels is potentially of interest.

When Manchester coding is employed, then relative to the NRZ sequence, the Manchester waveform has  $3/2$  as many transitions. Thus, since the SNR degradation due to asymmetry is directly related to the average transition density of the data sequence, one would intuitively expect that, for the same asymmetry, the Manchester case should yield a larger SNR degradation than the corresponding NRZ case. Whether or not and to what extent the above intuitive notion is indeed true depends on how one defines percent asymmetry for the Manchester case.

To demonstrate this point, consider the NRZ sequence of Figure 1 and the corresponding asymmetric Manchester waveforms which, for the previous asymmetry models are illustrated in Figure 2. Here, corresponding to Model 1,  $\Delta/2$  denotes the fractional (relative to the half-symbol time  $T/2$ ) elongation of the positive half pulse in the Manchester waveform, and for Model 2,  $\delta$  is accordingly defined relative to the same half-pulse width. Then, defining asymmetry as was done for the NRZ case but now relative to the half-pulse duration gives (for Model 1)

$$\text{Asymmetry} \triangleq n = \frac{\frac{T}{2}(1 + \Delta/2) - \frac{T}{2}(1 - \Delta/2)}{\frac{T}{2}(1 + \Delta/2) + \frac{T}{2}(1 - \Delta/2)} = \frac{\Delta}{2} \quad (6)$$

and, for Model 2,

$$\eta = \frac{\frac{T}{2}(1+2\delta) - \frac{T}{2}(1-2\delta)}{\frac{T}{2}(1+2\delta) + \frac{T}{2}(1-2\delta)} = 2\delta, \quad (7)$$

which are identical with (1) and (2).<sup>\*</sup> Once again, as in the NRZ case, the in-phase integrate-and-dump output depends, in general, on the polarity of the symbol over which it is integrating and on the preceding and succeeding symbols. Thus, evaluating this integrate-and-dump output for eight possible three-symbol sequences and noting that, for Model 1, the nominal bit synchronization lock-up misalignment is now  $\Delta T/8$ , we get an expression for the average probability of error corresponding to asymmetric Manchester random data, namely,

$$P_E = \frac{1}{4} \operatorname{erfc} \left[ \sqrt{E_s/N_0} (1 - \eta) \right] + \frac{1}{4} \operatorname{erfc} \left[ \sqrt{E_s/N_0} \left(1 - \frac{\eta}{2}\right) \right]. \quad (8)$$

Using (8) and (3), Figure 3 illustrates the SNR degradation in dB versus percent asymmetry for Manchester and, for comparison, NRZ data at  $E_s/N_0 = 1.5$  dB. Here note that the Manchester code yields a larger SNR degradation than NRZ for small asymmetry values, while the reverse is true for large percent asymmetries.

If, on the other hand, we define data asymmetry relative to the symbol time  $T$  for both NRZ and Manchester data, then equal percent asymmetry implies equal amounts of asymmetry (in seconds) as measured by the actual time displacements of the waveform transitions. Thus, for Manchester data, we have  $\eta = \Delta/4$  for Model 1 and  $\eta = \delta$  for Model 2. The corresponding expression for error probability is identical to (8) with  $\eta$  replaced by  $2\eta$ . Using this definition, Figure 4 also contains a plot of SNR degradation in dB versus percent asymmetry for  $E_s/N_0 = 1.5$  dB and Manchester data. Note that now the Manchester case always yields a larger SNR degradation for a given percent asymmetry. The conclusion to be reached here is that, in making comparisons between asymmetric NRZ and Manchester systems, one must exercise care in selecting a definition which is appropriate to the particular application at hand.

---

<sup>\*</sup> Note that while this definition allows for equal percent asymmetry when compared with NRZ, the actual time asymmetry (as measured in seconds) is different for the two cases. For equal time asymmetry, as would result if and Manchester sequence were processed by identical physical systems, the percent asymmetry for Manchester would be twice as high as for NRZ.

## THE EFFECT OF D.C. RESTORATION ON ERROR PROBABILITY PERFORMANCE IN THE PRESENCE OF ASYMMETRY

The investigation of the effects of d.c. restoration\* on communication link performance was prompted by test results [5] conducted in the Electronic Systems Test Laboratory (ESTL) at JSC which indicated significantly less performance degradation than that predicted by the analytic results of the previous sections. In particular, it was found that d.c. restoration tends to reduce the degrading effects of data asymmetry and thus it was necessary to incorporate d.c. restoration into the analytical model.

The effect of d.c. restoration on data detection is most easily accounted for by artificially shifting the decision threshold (nominally at zero) against which the matched filter output is compared. The amount of this artificial shift in threshold depends upon the specific way in which d.c. restoration comes about.

The simplest method of achieving d.c. restoration is to capacitively couple the input signal to the symbol synchronizer. In this case, the artificial threshold shift equals the d.c. component of the asymmetric data waveform in front of the capacitor which, for random data with transition density  $D$ , is easily shown to be

$$\Delta_t = \eta D \sqrt{E_s/T} \quad (9)$$

where  $\sqrt{E_s/T}$  is the data pulse amplitude in Figure 1. Computing the matched filter output for the eight possible three-symbol sequences made up of the present, preceding, and succeeding symbols and shifting these outputs by  $\Delta_t$  gives the result for the error probability performance of asymmetric NRZ data with d.c. restoration by capacitive coupling, namely,

$$P_E = \frac{1}{4} \operatorname{erfc} \left[ \sqrt{E_s/N_0} (1 - \eta D) \right] + \frac{1}{16} \operatorname{erfc} \left[ \sqrt{E_s/N_0} (1 - 2\eta + \eta D) \right] + \frac{1}{8} \operatorname{erfc} \left[ \sqrt{E_s/N_0} (1 - \eta + \eta D) \right] + \frac{1}{16} \operatorname{erfc} \left[ \sqrt{E_s/N_0} (1 + \eta D) \right] \quad (10)$$

For equiprobable data symbols ( $D = 0.5$ ), (10) simplifies to

$$P_E = \frac{3}{8} \operatorname{erfc} \left[ \sqrt{E_s/N_0} \left(1 - \frac{\eta}{2}\right) \right] + \frac{1}{16} \operatorname{erfc} \left[ \sqrt{E_s/N_0} \left(1 - \frac{3\eta}{2}\right) \right] + \frac{1}{16} \operatorname{erfc} \left[ \sqrt{E_s/N_0} \left(1 + \frac{\eta}{2}\right) \right] \quad (11)$$

---

\* D.C. restoration refers to the process by which the d.c. value of the asymmetric data waveform is forced to zero.

Comparing (11) with (3), we observe that the asymmetry is reduced and the effect of d.c. restoration is to compensate for the data asymmetry by shifting the effective decision threshold away from the shortened symbols.

For a given value of asymmetry, the value of  $E_s/N_0$  required to obtain  $P_E$  [as computed from (11)] equal to  $10^{-5}$  can be calculated. Comparing this value of  $E_s/N_0$  with that obtained from (5) for the same  $P_E$  gives the SNR degradation for asymmetric NRZ data with d.c. restoration by capacitive coupling. Figure 4 illustrates this SNR degradation versus asymmetry along with the comparable results obtained from (3) corresponding to no d.c. restoration (direct coupling).

Another method of achieving d.c. restoration, which depends specifically on the symbol synchronizer implementation itself, is to require the matched filter quadrature output to have zero crossings at the center of each symbol period that starts with a data transition. In this case, the effective shift in decision threshold relative to its nominal (zero) value is [5].

$$\Delta_t = \eta \sqrt{E_s/T} . \quad (12)$$

Comparing (16) with (13), we can immediately conclude that the error probability for this method of d.c. restoration is given by (10) with  $D = 1$ , i.e.,

$$P_E = \frac{5}{16} \operatorname{erfc} \left[ \sqrt{E_s/N_0} (1 - \eta) \right] + \frac{1}{8} \operatorname{erfc} \left[ \sqrt{E_s/N_0} \right] + \frac{1}{16} \operatorname{erfc} \left[ \sqrt{E_s/N_0} (1 + \eta) \right] . \quad (13)$$

We observe the same effect of d.c. restoration which reduces the asymmetry

Again by determining those values of  $E_s/N_0$  required to obtain  $P_E = 10^{-5}$  for various values of asymmetry, one can compute the SNR degradation for d.c. restoration based on symbol timing. The results of these calculations are illustrated in Figure 5 along with experimental test results taken in the ESTL [5] for the sake of comparison. It is to be noted that the experimental results include the effects of bandlimiting, whereas the theory as predicted by (13) does not account for these effects. Furthermore, the data detector used in the experimental setup was not a true matched filter as is assumed for the analytical model. Surprisingly enough, however, the analytic and experimental results show reasonably good agreement. In the next section, we consider the combined effects of bandlimiting and asymmetry on the performance of a filter-sample type data detector which is a more realistic model of the detector used in the ESTL tests.

## ERROR PROBABILITY PERFORMANCE (GATED INTEGRATE-AND-DUMP FILTER)

This section deals with another implementation of a data detector for asymmetric data, namely, the gated integrate-and-dump filter (see Figure 6). The motivation for studying the performance of such a detector stems from several considerations. First, from an implementation point of view, the gated integrate-and-dump has the advantage that operation at high data rates can be accomplished with smaller circuit losses than the ideal integrate-and-dump since the constraint on its switching times at the symbol transition instants can now be considerably relaxed. Second, since the input data stream possesses asymmetry, the ideal integrate-and-dump is no longer necessarily the optimum detector, and it is thus possible that an alternate (possibly simpler to implement) detector could yield superior performance.

Only the case of NRZ data is treated; however, as before, the results are obtained using no d.c. restoration and d.c. restoration by capacitive coupling. The numerical results presented permit a tradeoff between additional SNR degradation in the absence of asymmetry and an improvement in performance when asymmetry is high.

When the input data is random, then the output of the gated integrate-and-dump (GI&D) depends, in general, on the polarity of the symbol over which it is integrating and that of the preceding and succeeding symbols. Thus, one must compute these outputs for each of the eight possible three-symbol sequences (analogous to the approach taken in Sections for the ideal integrate-and-dump) and their corresponding conditional error probabilities. Then averaging these conditional error probabilities over the equal probabilities of the eight three-symbol sequences gives the average error probability performance of the GI&D detector.

In the absence of d.c. restoration, the average error probability performance of the gated integrate-and-dump is given by

$$P_E = \begin{cases} \frac{5}{16} \operatorname{erfc} \left[ \sqrt{E_s/N_0} (1 - 2\epsilon) \right] + \frac{1}{8} \operatorname{erfc} \left[ \sqrt{E_s/N_0} \left( \frac{1 - \eta}{\sqrt{1 - 2\epsilon}} \right) \right] \\ \quad + \frac{1}{16} \operatorname{erfc} \left[ \sqrt{E_s/N_0} \left( \frac{1 - 2\eta + 2\epsilon}{\sqrt{1 - 2\epsilon}} \right) \right]; & 0 \leq \epsilon \leq \eta/2 \\ \frac{1}{2} \operatorname{erfc} \left[ \sqrt{E_s/N_0} (1 - 2\epsilon) \right]; & \eta/2 \leq \epsilon \leq 1/2 . \end{cases} \quad (14)$$

where  $\epsilon$  is the fractional (relative to  $T$ ) gated interval at each end of the symbol. Figure 7 is a plot of  $P_E$  versus  $\epsilon$  with  $\eta$  as a parameter and  $E_s/N_0 = 9.6$  dB (corresponding to  $P_E = 10^{-5}$  when  $\epsilon = \eta = 0$ ). We observe from this figure that, for a given value of data asymmetry  $\eta$ ,  $P_E$



is minimized by choosing  $\epsilon = \eta/2$ . Figure 8 is an illustration of the symbol energy-to-noise ratio (in dB) required to achieve an average error rate of  $10^{-5}$  in the presence of data asymmetry. The curve labeled  $\epsilon=0$  corresponds to the performance of the ideal I&D. The remaining curves indicate a constant  $E_s/N_0$  for values of  $\eta \leq 2\epsilon$  in accordance with the second equation of (14) followed by an increase in  $E_s/N_0$  with  $\eta$  as required by the first equation of (14). Note that each of these curves crosses the  $\epsilon=0$  curve at some value of  $\eta$ , say  $\eta_0$ , which means that for  $\eta < \eta_0$ , the GI&D outperforms the ideal I&D in the sense of requiring less  $E_s/N_0$  for a given average probability of error. The dashed curve in Figure 8 represents the performance corresponding to selecting  $\epsilon = \eta/2$  at each value of  $\eta$  and is thus the best achievable with the GI&D.

When d.c. restoration by capacitive coupling is present, then the analogous result to (14) is

$$P_E = \begin{cases} \frac{1}{4} \operatorname{erfc} \left[ \sqrt{E_s/N_0} (1-2\epsilon)(1-\eta D) \right] + \frac{1}{16} \operatorname{erfc} \left[ \sqrt{E_s/N_0} (1-2\epsilon)(1+\eta D) \right] \\ + \frac{1}{16} \operatorname{erfc} \left[ \sqrt{E_s/N_0} \left( \frac{1-2\eta+\eta D+2\epsilon(1-\eta D)}{\sqrt{1-2\epsilon}} \right) \right] \\ + \frac{1}{8} \operatorname{erfc} \left[ \sqrt{E_s/N_0} \left( \frac{1-\eta+\eta D-2\epsilon\eta D}{\sqrt{1-2\epsilon}} \right) \right]; & 0 \leq \epsilon \leq \eta/2 \\ \frac{1}{4} \operatorname{erfc} \left[ \sqrt{E_s/N_0} (1-2\epsilon)(1-\eta D) \right] + \frac{1}{4} \operatorname{erfc} \left[ \sqrt{E_s/N_0} (1-2\epsilon)(1+\eta D) \right]; & \eta/2 \leq \epsilon \leq 1/2. \end{cases} \quad (15)$$

Figure 9 again illustrates  $P_E$  versus  $\epsilon$  with  $\eta$  as a parameter and  $E_s/N_0 = 9.6$  dB, where  $P_E$  is now computed from (15). We observe from this figure that, for a given value of data asymmetry, there exists a value of  $\epsilon$  which minimizes  $P_E$ ; however, unlike Figure 7, this value of  $\epsilon$  namely,  $\epsilon_{\min}$ , is not equal to  $\eta/2$ . Figure 10 is the analogous figure to Figure 8 when d.c. restoration is present. Again, the dashed curve corresponds to  $\epsilon = \epsilon_{\min}$  which represents the best achievable performance using gated integrate-and-dump as a data detector. Comparing Figure 10 with Figure 8, we observe the considerable reduction in SNR degradation due to data asymmetry when d.c. restoration is employed. This improvement is analogous to that achieved when other types of data detectors are used.

In conclusion, the use of a gated integrate-and-dump filter for detection of asymmetric NRZ data can, depending upon the amount of data asymmetry present, produce significant improvement in error rate performance, relative to that of an ideal integrate-and-dump filter.

## CONCLUSIONS

The SNR degradation due to data asymmetry in NRZ and Manchester uncoded and convolutionally encoded data streams has been systematically analyzed. A suitable asymmetry model was developed and error probability performance for two typical types of data detectors with or without d.c. restoration was derived. It was shown that the performance of detectors with d.c. restoration is always better than those without d.c. restoration.

As discussed in [1], to reduce data asymmetry degradation to a controllable amount, the Orbiter Ku-band signal processor has been modified by incorporating a compensated clock regenerator with an improved modulator driver into the interface circuits. This modification results in the overall data asymmetry for the Shuttle 50 Mbps channel to normally be less than 10%, and the resulting SNR degradation should be less than 0.5 dB even with a conventional I&D data detector. Should the asymmetry be greater than 10%, the SNR degradation would then be dependent on the type of the detector to be used.

## REFERENCE:

- [1] R. H. Cager, D. T. LaFlame, and L. C. Parode, "Orbiter Ku-band Integrated Radar and Communications Subsystem," to be published in IEEE Transactions on Communications.
- [2] G. K. Huth, "Integrated Source and Channel Encoded Digital Communication System Study," Final Report (No. R7607-3) under contract NAS 9-15240, July 31, 1976, Axiomatix, Marina del Rey, California.
- [3] R. S. Orr. "The Impact of Data Asymmetry on Bit Error Performance," Stanford Telecommunications, Inc., Technical Report (prepared under Subcontract No. 7023 to Operations Research, Inc., in support of Prime Contract No. NAS 5-23841 to NASA/GSFC), July 21, 1977.
- [4] W. K. Alem, G. K. Huth, and M. K. Simon; "Integrated Source and Channel Encoded Digital Communication System Design Study," Final Report (R7803-7) under Contract NAS 9-15240, March 31, 1978, Axiomatix, Marina del Rey, California.
- [5] J. W. Seyl and A. D. Travis, "Shuttle Communications Systems Compatibility and Performance Testing", to be published in IEEE Transaction on Communications.

|         |           | $\Delta E_s/N_o$ , dB |     |     |     |     |
|---------|-----------|-----------------------|-----|-----|-----|-----|
|         |           | 5%                    | 10% | 15% | 20% | 25% |
| $P_E^o$ | $\eta$    |                       |     |     |     |     |
|         | $10^{-2}$ | 0.2                   | 0.6 | 1.1 | 1.7 | 2.7 |
|         | $10^{-3}$ | 0.2                   | 0.7 | 1.4 | 2.5 | 2.9 |
|         | $10^{-4}$ | 0.3                   | 0.9 | 1.8 | 3.0 | 4.6 |
|         | $10^{-5}$ | 0.3                   | 1.0 | 2.1 | 3.4 | 5.0 |
|         | $10^{-6}$ | 0.4                   | 1.2 | 2.3 | 3.6 | 5.2 |

**Table 1. SNR Degradation Due to Asymmetry for Uncoded Random NRZ Data**

|           |                | $\Delta E_s/N_o$ , dB |     |     |     |     |
|-----------|----------------|-----------------------|-----|-----|-----|-----|
|           |                | 3%                    | 7%  | 10% | 15% | 20% |
| $P_b$     | $E_s/N_o$ (dB) |                       |     |     |     |     |
|           | $10^{-3}$      | 0.0                   | 0.1 | 0.3 | 0.5 | 0.8 |
|           | $10^{-4}$      | 0.8                   | 0.1 | 0.3 | 0.5 | 0.8 |
| $10^{-5}$ | 1.5            | 0.1                   | 0.3 | 0.5 | 0.9 | 1.3 |

**Table 2. SNR Degradation Due to Asymmetry for Rate  $\frac{1}{2}$  Convolutionally Encoded Random NRZ Data**

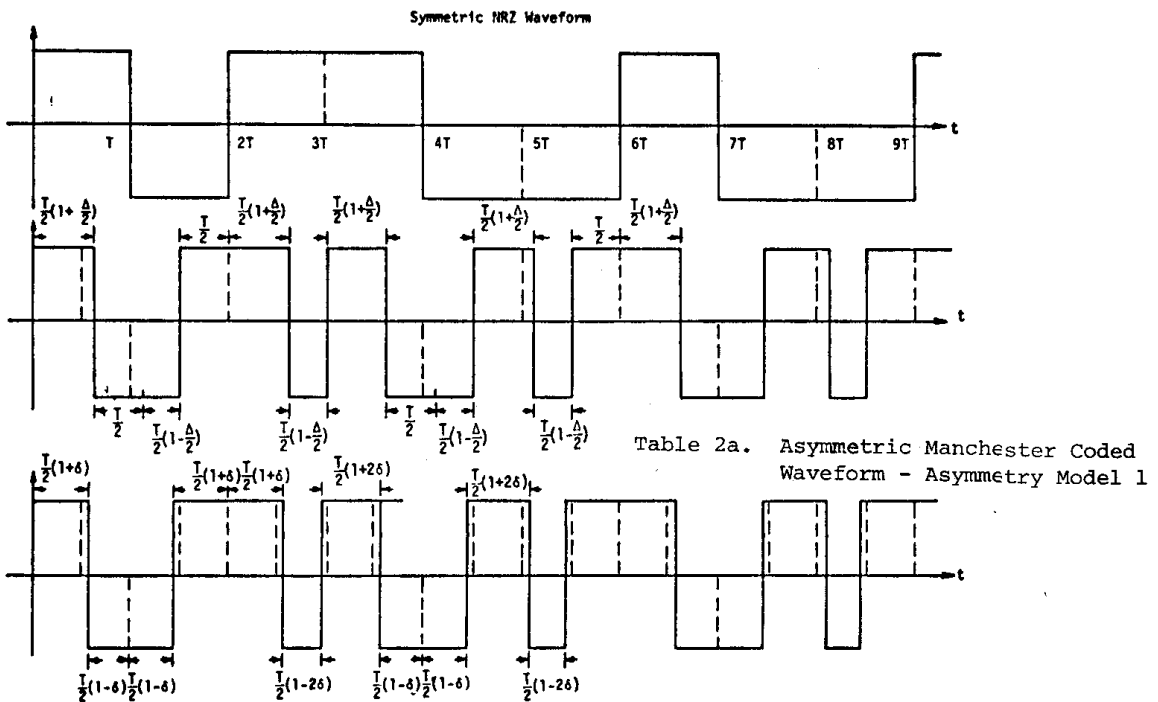
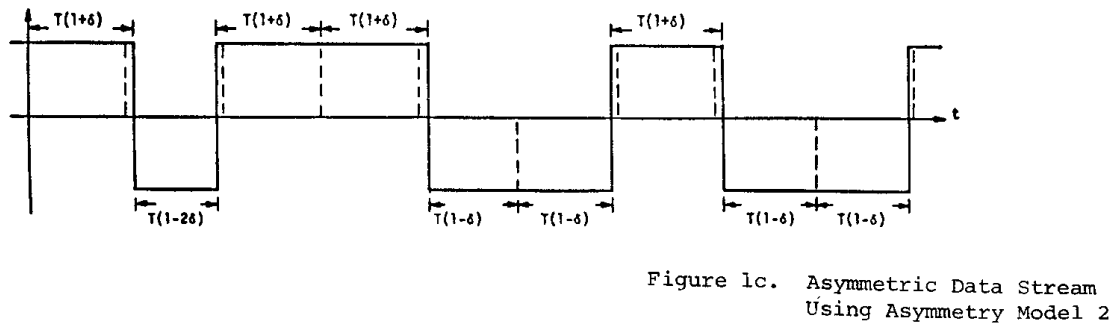
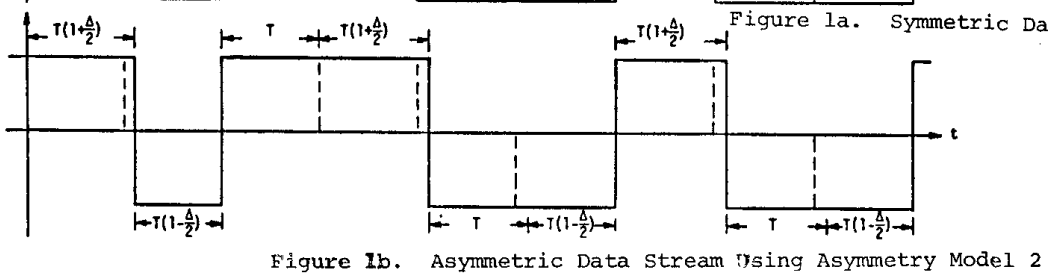
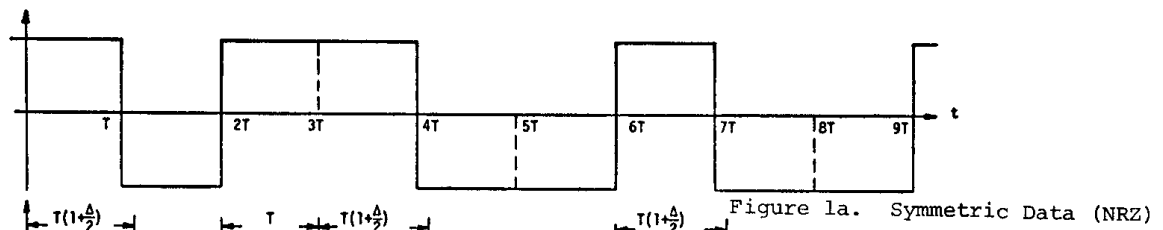


**Figure 2b. Asymmetric Manchester Coded Waveform - Asymmetry Model 2**

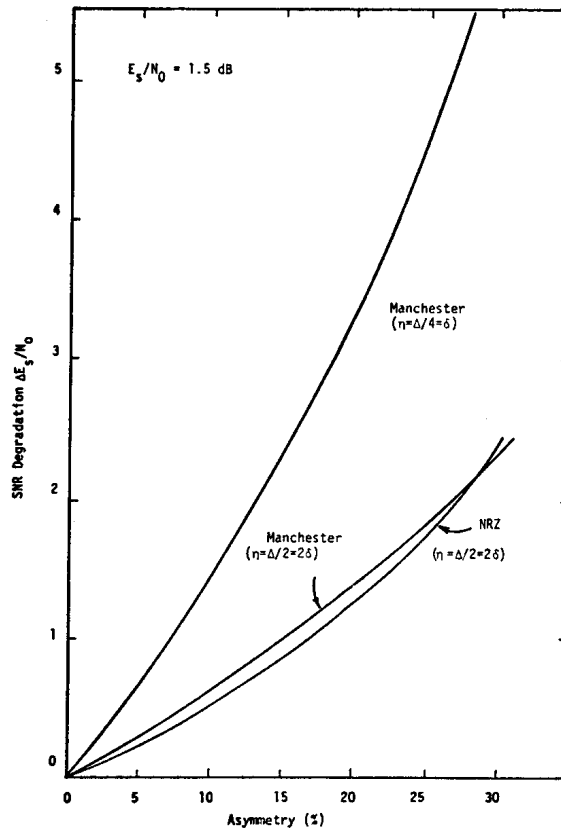


Figure 3. SNR Degradation vs. Percent Asymmetry for Random Manchester and NRZ Coded

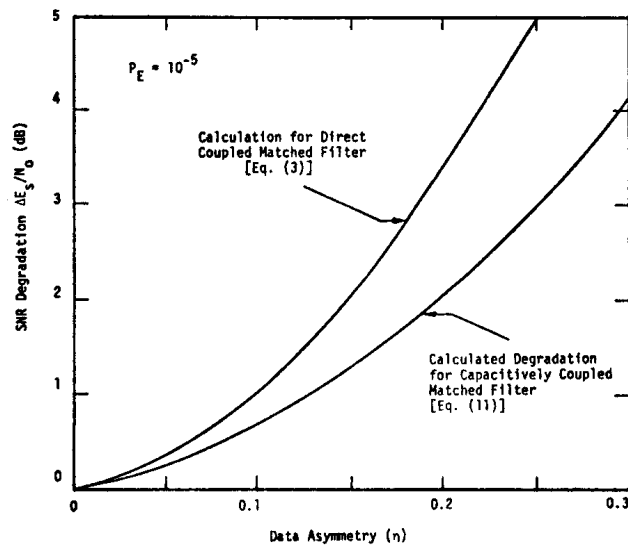
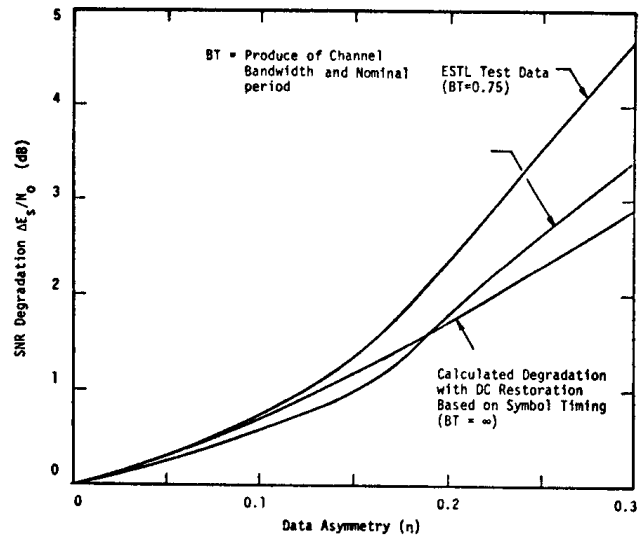
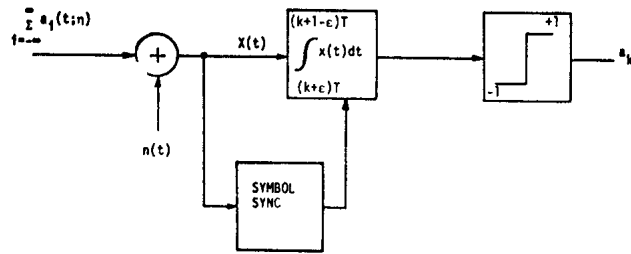


Figure 4. Performance Degradation Comparison for Direct Coupled and Capacitively-Coupled Matched -Filters; Random NRZ Data ( $D = 0.5$ )



**Figure 5. Performance Degradation for DC Restoration Based on Symbol Timing (NRZ data)**



**Figure 6. Gated Integrate-and-Dump Filter**

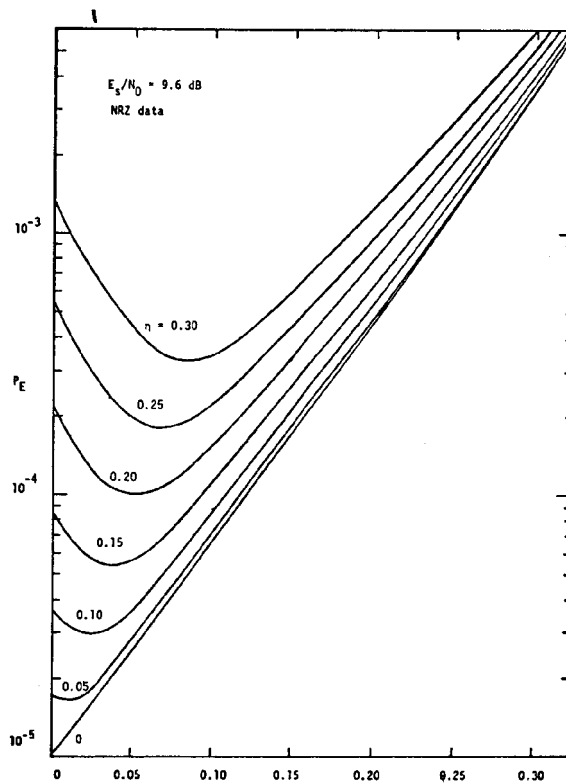


**Figure 7. Average Error Probability versus Gate Interval at Symbol Edge with Data Asymmetry as a Parameter - No D.C. Restoration**

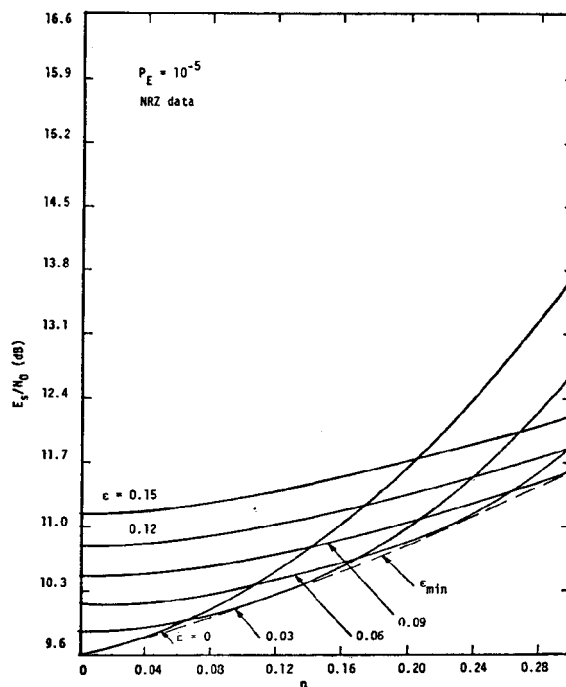


**Figure 8. Symbol Energy-to-Noise Ratio versus Data Asymmetry with Gate Interval at Symbol Edge as a Parameter - No D.C. Restoration**

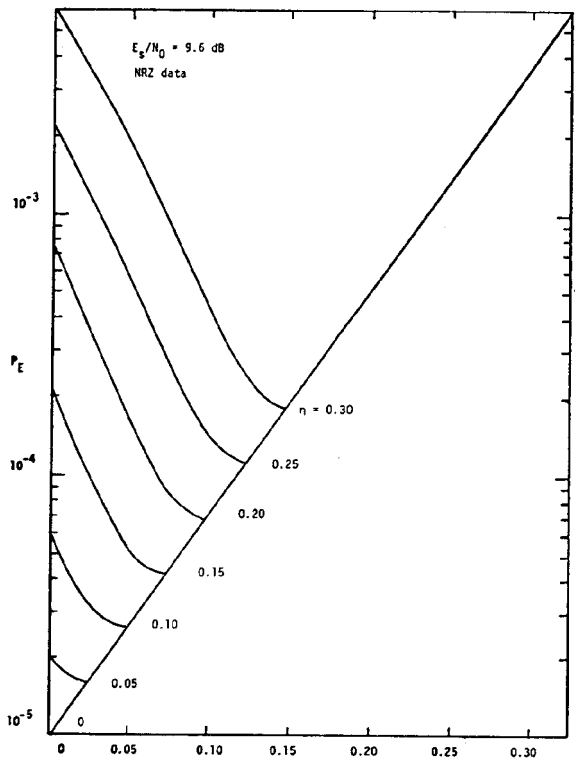


**Figure 9. Average Error Probability versus Gate Interval at Symbol Edge with Data Asymmetry as a Parameter - D.C. Restoration by Capacitive Coupling**

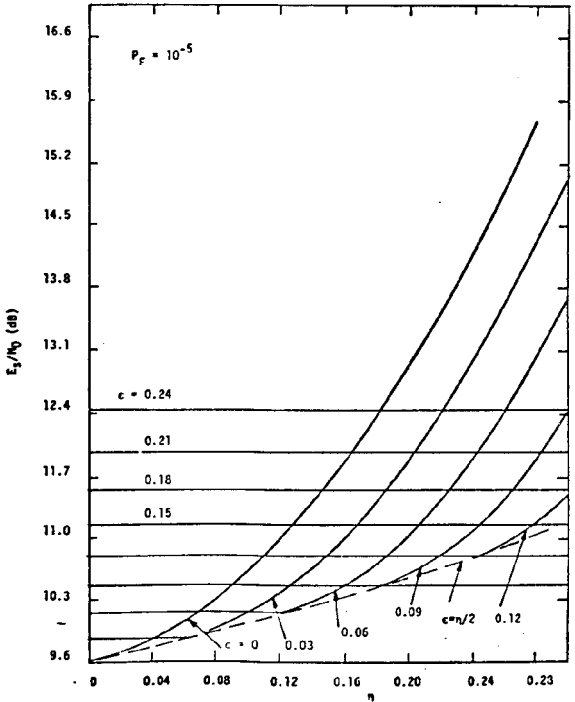


**Figure 10. Symbol Energy-to-Noise Ratio versus Data Asymmetry with Gate Interval at Symbol Edge as a Parameter - D.C. Restoration by Capacitive Coupling**